Crystallization and X-ray diffraction analysis of salicylate synthase, a chorismate-utilizing enyme involved in siderophore biosynthesis

James F. Parsons,[a]* Katherine Shi,[a] Kelly Calabrese[a] and Jane E. Ladner[a,b]

[a]Center for Advanced Research in Biotechnology, The University of Maryland Biotechnology Institute, 9600 Gudelsky Drive, Rockville, MD 20850, USA, and [b]National Institute of Standards and Technology, USA

Correspondence e-mail: parsonsj@umbi.umd.edu

Bacteria have evolved elaborate schemes that help them thrive in environments where free iron is severely limited. Siderophores such as yersiniabactin are small iron-scavenging molecules that are deployed by bacteria during iron starvation. Several studies have linked siderophore production and virulence. Yersiniabactin, produced by several *Enterobacteriaceae*, is derived from the key metabolic intermediate chorismic acid *via* its conversion to salicylate by salicylate synthase. Crystals of salicylate synthase from the uropathogen *Escherichia coli* CFT073 have been grown by vapour diffusion using polyethylene glycol as the precipitant. The monoclinic ($P2_1$) crystals diffract to 2.5 Å. The unit-cell parameters are $a = 57.27$, $b = 164.07$, $c = 59.04$ Å, $\beta = 108.8°$. The solvent content of the crystals is 54% and there are two molecules of the 434-amino-acid protein in the asymmetric unit. It is anticipated that the structure will reveal key details about the reaction mechanism and the evolution of salicylate synthase.

1. Introduction

Yersiniabactin is a siderophore first identified in *Yersinia*, but produced by a number of pathogenic *Enterobacteriaceae* including certain *Escherichia coli* strains (Schubert *et al.*, 1998). Siderophores are small iron-chelating molecules that bacteria produce and deploy in order to acquire the necessary ferric iron from host environments where free iron is extremely limited (Gehring *et al.*, 1998). The iron affinity of siderophores is very high, with dissociation constants of $\leq 10^{-30} M$ being common. The genes encoding yersiniabactin production reside on the $\sim$40 kDa high-pathogenicity island (HPI) located on the *Yersinia* genome and on similar genetic elements in other species (Schubert *et al.*, 2004). The HPI and yersiniabactin production are both conclusively linked to virulence in several organisms (Schubert *et al.*, 2002).

Salicylic acid serves as the initial building block for yersiniabactin (Fig. 1) and it is synthesized from chorismic acid by salicylate synthase (SS), also known as Irp9 (iron-repressible protein) and YbtS (Kerbarh *et al.*, 2005; Pelludat *et al.*, 2003). A similar protein known as MbtI (37% identical to SS) functions in the biosynthesis of myco-
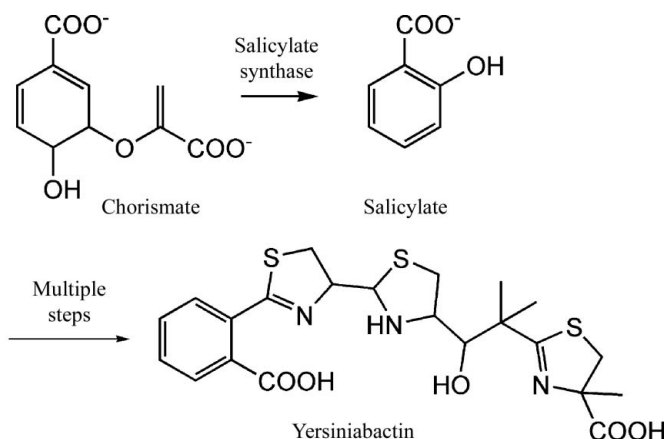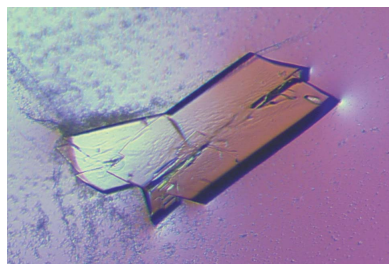

Figure 1
The reaction catalyzed by salicylate synthase and the subsequent incorporation of salicylate into yersiniabactin.

271

bactin, a siderophore produced by *Mycobacterium tuberculosis*. MbtI has also been crystallized and may also be a salicylate synthase (Harrison *et al.*, 2005). In other known instances of bacterial salicylate production, two enzymes are typically involved: isochorismate synthase and isochorismate lyase. Therefore, it is of interest to examine the structure of SS in order to detail the mechanism of the SS-catalyzed conversion of chorismate to salicylate. It is clear from sequence analysis that SS is an anthranilate synthase homolog. The C-terminal 260 residues of the 434-amino-acid protein are ~36% identical to known anthranilate synthases. However, the N-terminal portion of the sequence bears little similarity to known sequences. The crystal structure will therefore be revealing in terms of the role of the N-terminal 170 residues in catalysis as well as its evolutionary origin, particularly regarding the relationship of SS to other chorismate-utilizing enzymes such as anthranilate synthase and *p*-aminobenzoate synthase (Parsons *et al.*, 2002; Spraggon *et al.*, 2001)

2. Materials and methods

2.1. Cloning and expression of salicylate synthase

The DNA encoding SS was amplified from *E. coli* CFT073 genomic DNA (ATCC)[1] by PCR using KOD polymerase (Novagen) and synthetic primers compatible with the sequence of the gene encoding SS described in the TIGR Comprehensive Microbial Resource database (locus c2419 in the CFT073 sequence; http://cmr.tigr.org). The amplified fragment encoding SS was digested with the restriction enzymes *Nde*I and *Hin*dIII and ligated into the similarly digested expression vectors pET21a and pET28a, yielding clones for expression of native and His-tagged SS.

E. coli strain BL21(DE3) was used for the expression of both native and His-tagged proteins. Cells transformed with pET28a-SS were grown in ZYP-5052 autoinduction medium supplemented with 200 µg ml^{-1} kanamycin at 308 K (Studier, 2005). Cells were harvested after reaching saturation, usually at an optical density of ~11 at 600 nm and typically after 14–17 h. Native protein was expressed from pET21a-SS in a similar manner except that the media contained 100 µg ml^{-1} ampicillin instead of kanamycin. Selenomethionine-labeled SS was expressed using pET21a-SS, *E. coli* strain B834(DE3) and defined autoinduction media suitable for selenomethionine labeling. In all cases, cells were harvested by centrifugation and lysed by sonication. All steps were performed on ice or at 277 K except for the chromatographic steps for native SS, which were performed at room temperature.

His-tagged SS was purified by Ni^{2+}-ion affinity chromatography as directed by the resin manufacturer (Novagen). The His tag was removed by human α-thrombin (Hematologic Technologies), yielding SS with an additional Gly-Ser-His sequence prior to the N-terminal Met of the native sequence. The cleaved tag was removed from solution by a second pass over the Ni^{2+} column and the thrombin was removed using benzamidine agarose. Purified cleaved SS was dialyzed against 50 m*M* HEPES, 1 m*M* EDTA, 1 m*M* DTT pH 7.6, concentrated to ~16 mg ml^{-1} and stored at 193 K. The yield was about 40 mg pure enzyme per litre of culture. Native SS eventually yielded the best crystals and was purified in the following manner. Cells were sonicated in 50 m*M* Tris, 5 m*M* EDTA, 2 m*M* DTT,

300 m*M* NaCl pH 8.0. Insoluble cell material was removed by centrifugation (30 min at 35 000*g*). SS was precipitated from the crude supernatant by the addition of solid ammonium sulfate to 45%(*w*/*v*). This material, containing precipitated SS, was resuspended in 50 m*M* Tris, 2 m*M* DTT pH 8.0 and dialyzed against 2 × 2 l of the same buffer. The desalted dialysate was then applied onto a 56 ml HQ50 (Poros) anion-exchange column in 50 m*M* Tris pH 8.0 and eluted with a linear gradient of sodium chloride in 50 m*M* Tris pH 8.0. Fractions containing SS were pooled, dialyzed against 2 l 25 m*M* Tris, 2 m*M* DTT pH 8.3 and concentrated to <10 ml before being applied onto a 10 ml high-resolution HQ20 anion-exchange column equilibrated with the same buffer. A linear gradient of sodium chloride was again used to elute SS from the column. The desired fractions were pooled, concentrated to <10 ml and dialyzed against 25 m*M* MOPS, 2 m*M* DTT pH 6.8 before being applied onto a 25 ml HS20 cation-exchange column equilibrated with 25 m*M* MES pH 6.3. After elution with sodium chloride, the purest fractions were pooled, dialyzed against 25 m*M* MOPS, 2 m*M* DTT, 5 m*M* MgCl$_2$ pH 7.2, concentrated to 15 mg ml^{-1} and stored at 193 K. Selenomethionine-containing SS was produced in a similar manner except the strain used for expression was *E. coli* B834(DE3). Yields of SeMet SS were reduced by about 50% compared with unlabeled preparations.

2.2. Crystallization of salicylate synthase

Initial screening with affinity-purified SS identified two conditions that yielded crystals. The first condition, Hampton Index Screen
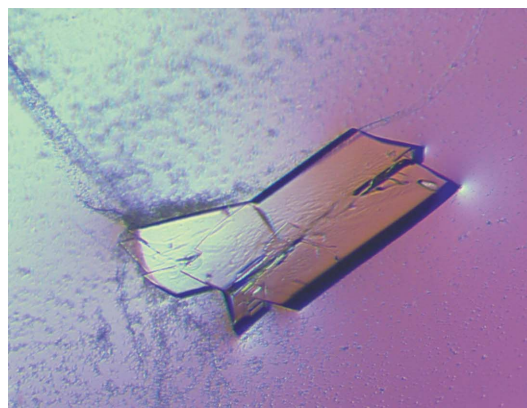
(a)
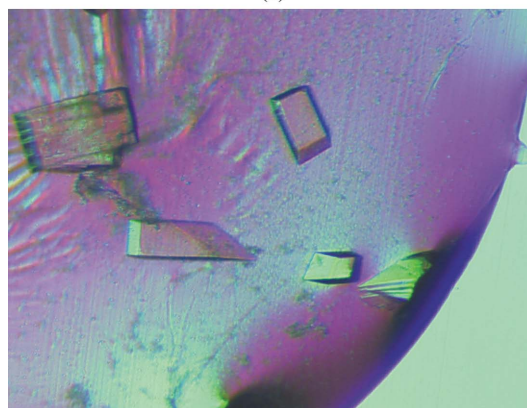
(b)

Figure 2
Crystals of salicylate synthase. (*a*) Larger twinned plate-like crystals grown from polyacrylic acid. This crystal is ~1 mm in its largest dimension. (*b*) Smaller higher quality crystals grown from polyethylene glycol and in the presence of detergent (see text). These crystals are about 0.2 mm in their largest dimension

---

[1] Certain commercial materials, instruments and methods are identified in this manuscript in order to specify the experimental procedure as completely as possible. In no case does such identification imply a recommendation or endorsement by the National Institute of Standards and Technology, nor does it imply that the material, instrument or equipment identified is necessarily the best available for the purpose.

Table 1
Crystal parameters and data-processing statistics.

Values in parentheses are for the highest resolution shell.

Space group	$P2_1$
Unit-cell parameters (Å, °)	$a = 57.27$, $b = 164.07$, $c = 59.04$, $\beta = 108.8$
Resolution range (Å)	29.8–2.5 (2.6–2.5)
Total reflections	264183 (22758)
Unique reflections	68924 (6007)
Completeness	98.1 (98.1)
R_{merge} (%)	11.6 (33.6)
Mean $I/\sigma(I)$	8.2 (2.4)
Redundancy	3.8 (3.8)
Solvent content (%)	54
Molecules per ASU	2

reagent No. 59 (22% polyacrylic acid 5100, 0.2 M MgCl$_2$, 0.05 M HEPES pH 7.5), yielded large (0.5–1 mm in the two larger dimensions; Fig. 2a) plates. The second condition, Hampton PEG/Ion Screen reagent No. 25 (20% PEG 3350, 0.2 M magnesium acetate), yielded smaller crystals of variable morphology (Fig. 2b). Attempts to optimize the first condition gave mixed results. Crystals could be reliably obtained, but only a small percentage of them diffracted appreciably; most gave no diffraction. Ultimately, this condition was abandoned; however, we did collect a single 2.7 Å data set from crystals grown using polyacrylic acid as the precipitant. The second condition, which initially looked less promising, improved significantly upon optimization. Manual screens varying the buffer, pH, PEG molecular weight, protein concentration and magnesium salt were examined. The best conditions identified by optimization were 14–18% PEG 8000, 0.2 M magnesium acetate, 0.1 M Tris, 5 mM chorismate pH 8.0 and a protein concentration of ∼16 mg ml^{-1} prior to mixing. Crystals formed from hanging or sitting drops within 72–96 h at ambient temperature. Crystals were improved further after screening 72 detergents (Hampton Detergent Kits 1, 2 and 3). Screening wa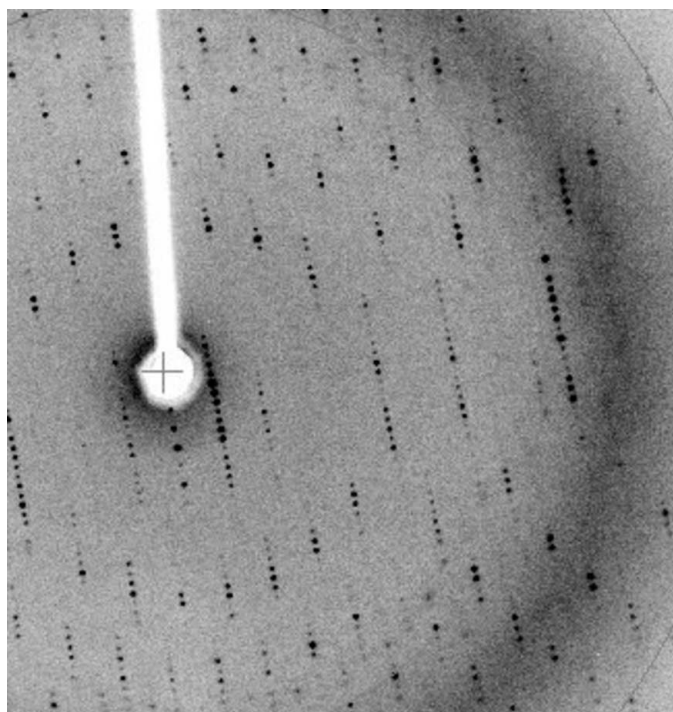s carried out in 24-well hanging-drop plates with one column (four wells) per detergent. 15 µl SS was mixed with 15 µl 14% PEG 3350, 0.2 M magnesium acetate, 0.1 M Tris pH 8.0 and 3 µl detergent as supplied in the kit. 3.5 µl drops of this mixture were equilibrated against wells containing the above solution and PEG 3350 at 14–17%. Lauryldimethylamine oxide and nonyl-β-D-thiomaltoside were judged to be most effective at enhancing crystal morphology and were used in subsequent experiments. Crystals are therefore optimally grown by mixing equal amounts of a protein solution containing 16 mg ml^{-1} SS, 50 mM Tris pH 8.0, 5 mM chorismate and 150 M nonyl-β-D-thiomaltoside (or 100 µM lauryldimethylamine oxide) with a well solution containing 14% PEG 3350, 0.2 M magnesium acetate, 0.1 M Tris pH 8.0. 3.5 µl drops of this mixture were equilibrated at room temperature (∼295 K) against wells containing 1 ml 14–17% PEG 3350, 0.2 M magnesium acetate, 0.1 M Tris pH 8.0.

2.3. Diffraction analysis

Crystals were transferred to a cryoprotectant solution consisting of the well solution and 50% PEG 8000 in a 1:1 ratio or were mounted using immersion or paraffin oil. Diffraction experiments were carried out using a Rigaku MicroMax 007 rotating-anode generator, an R-AXIS IV^{++} image-plate detector and an X-stream 2000 cryocooler (Fig. 3). *CrystalClear* (Pflugrath, 1999) was used for data collection and processing. An initial data set was collected and the statistics are shown in Table 1.

2.4. Laser light scattering

The solution molecular weight of SS was determined by a combination of laser light scattering and interferometric refractometry using a DAWN EOS and Optilab DSP system (Wyatt). Samples were subjected to gel-filtration chromatography (Shodex KW-802.5; 300 × 8 mm) prior to in-line analysis. Molecular weights were calculated using *ASTRA* software.

3. Conclusion

Salicylate synthase from the yersiniabactin-biosynthesis pathway in uropathogenic *E. coli* has been crystallized by vapour diffusion. The crystals diffract to at least 2.5 Å using a conventional rotating-anode X-ray source. A complete data set has been collected. Laser light-scattering experiments indicate that SS is a dimer in solution with a weight of ∼88.5 kDa. That this figure is less than the calculated weight of dimeric SS (∼97 kDa) suggests a possible monomer–dimer equilibrium. Analytical ultracentrifugation experiments are under way to examine this possibility. However, at the concentrations used for crystal growth it is likely that the dimer predominates. Furthermore, assuming the presence of an SS dimer in the asymmetric unit yields a reasonable Matthews coefficient of 2.74 Å^3 Da^{-1} and a solvent content of 55%. It is anticipated that once solved, the structure will reveal key information about how SS catalyzes the conversion of chorismate to salicylate, a conversion that in other organisms and pathways requires two enzymes (Gaille *et al.*, 2002).

Figure 3
Image showing typical diffraction from a crystal of salicylate synthase.

References

Gaille, C., Kast, P. & Haas, D. (2002). *J. Biol. Chem.* **277**, 21768–21775.
Gehring, A. M., DeMoll, E., Fetherston, J. D., Mori, I., Mayhew, G. F., Blattner, F. R., Walsh, C. T. & Perry, R. D. (1998). *Chem. Biol.* **5**, 573–586.

Harrison, A. J., Ramsay, R. J., Baker, E. N. & Lott, J. S. (2005). *Acta Cryst.* F**61**, 121–123.

Kerbarh, O., Ciulli, A., Howard, N. I. & Abell, C. (2005). *J. Bacteriol.* **187**, 5061–5066.

Parsons, J. F., Jensen, P. Y., Pachikara, A. S., Howard, A. J., Eisenstein, E. & Ladner, J. E. (2002). *Biochemistry*, **41**, 2198–2208.

Pelludat, C., Brem, D. & Heesemann, J. (2003). *J. Bacteriol.* **185**, 5648–5653.

Pflugrath, J. W. (1999). *Acta Cryst.* D**55**, 1718–1725.

Schubert, S., Picard, B., Gouriou, S., Heesemann, J. & Denamur, E. (2002). *Infect. Immun.* **70**, 5335–5337.

Schubert, S., Rakin, A. & Heesemann, J. (2004). *Int. J. Med. Microbiol.* **294**, 83–94.

Schubert, S., Rakin, A., Karch, H., Carniel, E. & Heesemann, J. (1998). *Infect. Immun.* **66**, 480–485.

Spraggon, G., Kim, C., Nguyen-Huu, X., Yee, M. C., Yanofsky, C. & Mills, S. E. (2001). *Proc. Natl Acad. Sci. USA*, **98**, 6021–6026.

Studier, F. W. (2005). *Protein Expr. Purif.* **41**, 207–234.